Spin Model of Magnetostrictions in Multiferroic Mn Perovskites

Masahito Mochizuki,[1] Nobuo Furukawa,[2,3] and Naoto Nagaosa[1,4]

[1]*Department of Applied Physics, The University of Tokyo, 7-3-1, Hongo, Bunkyo-ku, Tokyo 113-8656, Japan*
[2]*Department of Physics, Aoyama Gakuin University, Fuchinobe 5-10-1, Sagamihara, 229-8558 Japan*
[3]*Multiferroics Project, ERATO, Japan Science and Technology Agency (JST), c/o Department of Applied Physics, The University of Tokyo, 7-3-1, Hongo, Bunkyo-ku, Tokyo 113-8656, Japan*
[4]*Cross-Correlated Materials Research Group (CMRG) and Correlated Electron Research Group (CERG), RIKEN-ASI, Saitama 351-0198, Japan*

(Received 21 February 2010; published 16 July 2010)

We theoretically study origins of the ferroelectricity in the multiferroic phases of the rare-earth (R) Mn perovskites, $R\mathrm{MnO_3}$, by constructing a realistic spin model including the spin-phonon coupling, which reproduces the entire experimental phase diagram in the plane of temperature and Mn-O-Mn bond angle for the first time. Surprisingly we reveal a significant contribution of the symmetric ($\boldsymbol{S}\cdot\boldsymbol{S}$)-type magnetostriction to the ferroelectricity even in a spin-spiral-based multiferroic phase, which can be larger than the usually expected antisymmetric ($\boldsymbol{S}\times\boldsymbol{S}$)-type contribution. This explains well the nontrivial behavior of the electric polarization. We also predict the noncollinear deformation of the E-type spin structure and a wide coexisting regime of the E and spiral states, which resolve several experimental puzzles.

DOI: 10.1103/PhysRevLett.105.037205 PACS numbers: 75.80.+q, 75.10.Hk, 75.47.Lx, 75.85.+t

Frustrating spins in magnets often exhibit not only nontrivial orders but also intriguing switching and dynamical phenomena associated with phase competitions. Effective reduction of the spin-exchange energy due to the frustration increases the relative importance of other tiny interactions such as the Dzyaloshinskii-Moriya (DM) interaction, single-ion anisotropy, and spin-phonon coupling. Their fine energy balance results in a keen conflict of various states. This enables us to achieve sensitive phase controls and huge responses leading to new functionalities of materials, and also provides challenging issues for fundamental science.

The rare-earth (R) Mn perovskites, $R\mathrm{MnO_3}$, offer one of the most typical examples. In this class of materials, the nearest-neighbor spin exchange is very small ($\sim$1 meV) relative to that in other perovskite compounds (e.g., $\sim$15 meV in $\mathrm{LaTiO_3}$) due to the cancellation of exchange contributions from t_{2g} and e_g orbital sectors [1]. Consequently the next-neighbor antiferromagnetic (AFM) coupling becomes comparable to the nearest-neighbor ferromagnetic (FM) coupling. Their frustration gives rise to various competing phases including multiferroic phases where the frustration-induced nontrivial spin order generates ferroelectric polarization $\boldsymbol{P}$ [2,3].

Recent experiments revealed spectacular magnetoelectric (ME) phenomena in these multiferroic phases, i.e., magnetic-field-induced $\boldsymbol{P}$ flops [2,4], colossal magnetocapacitance [4–6], and electromagnons [7,8]. To study and/or control these cross correlation phenomena, thorough understanding of the magnetic structures, the phase competitions, and the coupling between magnetic and ferroelectric orders based on a reliable model is essential.

However, there still remain many experimental observations, which are not understood theoretically. (i) Multifurcation of the sinusoidal collinear phase at higher temperature (T) into four low-T phases depending on the ionic R-site radius (r_R) [9]. (ii) Nontrivial r_R dependence of the magnitude and direction of $\boldsymbol{P}$ [9]. (iii) Apparently contradicting neutron-scattering results on the magnetic commensurability in the compounds with small r_R [10–13]. (iv) Anomalous T dependence of $|\boldsymbol{P}|$ for $\mathrm{YMnO_3}$ and $\mathrm{ErMnO_3}$ [9].

In this Letter, we study theoretically the interplay of symmetric ($\boldsymbol{S}\cdot\boldsymbol{S}$)-type magnetostriction (MS) and antisymmetric ($\boldsymbol{S}\times\boldsymbol{S}$)-type MS in a realistic spin model for $R\mathrm{MnO_3}$, and resolve all the puzzles listed above. We find a large ($\boldsymbol{S}\cdot\boldsymbol{S}$) contribution to the ferroelectricity even in a spiral spin phase. This mechanism is generally expected in all the spin-spiral-based multiferroics. We start with a model in which the Mn $S=2$ spins are treated as classical vectors on a cubic lattice. A similar model has been examined in Refs. [1,14] which gives the transition between two types of multiferroic spiral spin phases and explains several ME phenomena quantitatively. Here we further include the lattice degrees of freedom. This enables us to study the effect of the ($\boldsymbol{S}\cdot\boldsymbol{S}$)-type MS as a source of the above puzzles, which has been missed thus far.

The Hamiltonian is given by

$$\mathcal{H}=\sum_{\langle i,j\rangle}J_{ij}\boldsymbol{S}_i\cdot\boldsymbol{S}_j+D\sum_i S_{\zeta i}^2+E\sum_i(-1)^{i_x+i_y}(S_{\xi i}^2-S_{\eta i}^2)+\sum_{\langle i,j\rangle}\boldsymbol{d}_{ij}\cdot(\boldsymbol{S}_i\times\boldsymbol{S}_j)+K\sum_i(\delta_{i,i+\hat{x}}^2+\delta_{i,i+\hat{y}}^2),\qquad(1)$$

where i_x, i_y, i_z represent the integer coordinates of the ith Mn ion with respect to the cubic x, y and z axes.

The first term describes the spin-exchange interactions as shown in Fig. 1(a). The second and third terms stand for the single-ion anisotropy. For the local axes $\boldsymbol{\xi}_i$, $\boldsymbol{\eta}_i$ and $\boldsymbol{\zeta}_i$

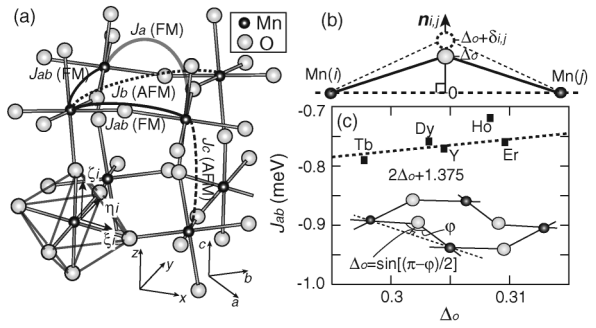

FIG. 1. (a) Spin exchanges in $R\mathrm{MnO_3}$ where FM (AFM) denotes (anti)ferromagnetic exchange. (b) Mn(i)-O-Mn(j) bond in the orthorhombic lattice and local vector $\boldsymbol{n}_{i,j}$. The O ion is displaced from its cubic position (0) to the orthorhombic position (Δ_o) at higher T. A further shift $\delta_{i,j}$ along $\boldsymbol{n}_{i,j}$ can be induced at low T via the spin-lattice coupling. (c) Δ_o vs J_{ab} for several R species calculated in Ref. [1]. Here Δ_o is normalized by the MnO bond length.

attached to each $\mathrm{MnO_6}$ octahedron, we use the structural data of $\mathrm{DyMnO_3}$ [15]. The fourth term denotes the DM interaction. The DM vectors $\boldsymbol{d}_{ij}$ are expressed using five DM parameters, α_{ab}, β_{ab}, γ_{ab}, α_c and β_c, as given in Ref. [16] because of the crystal symmetry. The last term represents the lattice elastic term with K being the elastic constant. Here $\delta_{i,j}$ is a shift of the O ion between ith and jth Mn ions normalized by the MnO bond length. Note that the O ion in the orthorhombic lattice is already displaced from its cubic position. We consider $\delta_{i,j}$ as a further shift from the position at higher T in the presence of magnetic order at low T.

Since the nearest-neighbor FM coupling in $R\mathrm{MnO_3}$ is sensitive to the Mn-O-Mn bond angle, we consider the Peierls-type spin-phonon coupling $J_{ij} = J_{ab} + J'_{ab}\delta_{i,j}$ for the in-plane Mn-O-Mn bonds where $J'_{ab} = \partial J_{ab}/\partial\delta$ [17]. We assume that the shift of O ion $\delta_{i,j}$ occurs along the local axis $\boldsymbol{n}_{i,j}$ directing from its cubic position (0) to the orthorhombic position (Δ_o) at higher T [see Fig. 1(b)]. Then the positive (negative) shift decreases (increases) the Mn-O-Mn bond angle.

The values of J_{ab}, J_c, J_b, D, E, and five DM parameters have been microscopically determined in Ref. [1] for several $R\mathrm{MnO_3}$ compounds. Except for J_b, they are nearly invariant upon the R-site variation in the vicinity of the multiferroic phases. We fix $J_{ab} = -0.8$, $J_c = 1.25$, $D = 0.2$, $E = 0.25$, $(\alpha_{ab}, \beta_{ab}, \gamma_{ab}) = (0.1, 0.1, 0.14)$, and $(\alpha_c, \beta_c) = (0.42, 0.1)$. Here the energy unit is meV. We also find that very weak FM exchange J_a is necessary to produce the E phase, and adopt $J_a = -0.1$. The value of K is chosen to be 500 so as to reproduce the experimental P in the E phase [see Fig. 3(a)]. We obtain the value of J'_{ab} from the Δ_o dependence of J_{ab} for several R species [see Fig. 1(c)], which gives $J'_{ab} = \partial J_{ab}/\partial\Delta_o = 2$.

We treat J_b as a variable which increases (decreases) as r_R decreases (increases). This is because the exchange path for J_b contains two O $2p$ orbitals, and the orthorhombic distortion, whose magnitude is controlled by r_R, enhances their hybridization. We find that overall features of the phase evolution upon the R-site variation are reproduced as a function of J_b even without considering the slight R dependence of other parameters.

We analyze the above model using the replica exchange Monte Carlo (MC) method [18]. Both spins and oxygen positions are updated in the simulation, and each exchange sampling is taken after 400 standard MC steps. Typically, we perform 600 exchanges for a system of $N = 48 \times 48 \times 6$ sites along x, y, and z axes with periodic boundaries. We identify transition points and spin structures from T profiles of specific heat and spin-helicity vector $\boldsymbol{h} = \frac{1}{2N}\sum_i(\boldsymbol{S}_i \times \boldsymbol{S}_{i+\hat{x}} + \boldsymbol{S}_i \times \boldsymbol{S}_{i+\hat{y}})/S^2$. We also calculate spin correlations in the momentum space.

We first display the theoretical T-J_b phase diagram in Fig. 2, which successfully reproduces the experimentally observed phase evolutions [19]. More concretely, the following four phases successively emerge at low T as J_b decreases: the A, ab-spiral, bc-spiral, and E phases. In the A (E) phase, the FM (up-up-down-down) Mn-spin layers stack antiferromagnetically, while in the ab (bc) spiral phase, the Mn spins rotate within the ab (bc) plane ($Pbnm$ setting) to form transverse cycloids [20,21]. As T decreases, these four phases emerge with multifurcation from the sinusoidal collinear phase at higher T where the collinear Mn spins are sinusoidally modulated in amplitude. The spin structure is commensurate (C) with $q_b = 0.5$ in the E phase, whereas it is incommensurate (IC) in the ab and bc spiral phases. Importantly, the sinusoidal collinear state is also IC even above the E phase (e.g., $q_b = 0.458$ for $J_b = 2.4$), and the spin-phonon coupling is a source of the IC-C transition with lowering T.

In the ab (bc) spiral phase, it has been naively believed that the antisymmetric ($\boldsymbol{S} \times \boldsymbol{S}$)-type MS induces the ferroelectric polarization $\boldsymbol{P} \parallel a$ ($\boldsymbol{P} \parallel c$) [22–24]. However, the observed P in the ab spiral phase is much larger than that in the bc spiral phase. For instance, the P_a in the ab spiral phase of $\mathrm{DyMnO_3}$ under $\boldsymbol{H} \parallel b$ is 2.5 times larger than P_c in the bc spiral phase at $H = 0$ [4,5]. Moreover, in

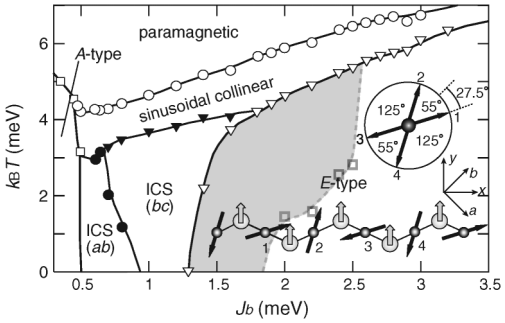

FIG. 2. Theoretical phase diagram of $R\mathrm{MnO_3}$ in the plane of J_b and T. Here ICS denotes the incommensurate spiral phase. In the shaded area, the E and ICS states can coexist. Inset shows real-space spin configuration of the E phase. Shifts of the O ions due to ($\boldsymbol{S} \cdot \boldsymbol{S}$)-type magnetostriction are shown by gray arrows.

$Eu_{0.6}Y_{0.4}MnO_3$, the P_a at $H = 0$ is approximately 10 times larger than P_c under $\boldsymbol{H} \parallel a$, which excludes the influence of f moments as its origin because of their absence [25]. This is quite puzzling since we expect nearly identical strength of the $(\boldsymbol{S} \times \boldsymbol{S})$-type MS in these two phases. Recent first-principles study also suggested different mechanisms of P between the two spiral phases [26]. To solve this issue, we calculate the polarization due to the $(\boldsymbol{S} \cdot \boldsymbol{S})$-type MS, $\boldsymbol{P}_S = (\tilde{P}_a, \tilde{P}_b, \tilde{P}_c)$ from the oxygen shifts. Because of the staggered local axes $\boldsymbol{n}_{i,j}$ on the zigzag Mn-O chain, $\tilde{P}_\gamma$ $(\gamma = a, b, c)$ is given by

$$\tilde{P}_\gamma = -\frac{\Pi_\gamma}{N}\sum_i [(-1)^{i_x+i_y+m}\delta_{i,i+\hat{x}} + (-1)^{i_x+i_y+n}\delta_{i,i+\hat{y}}],$$

where $(m, n) = (0, 0)$ for $\gamma = a$, $(m, n) = (1, 0)$ for $\gamma = b$, and $(m, n) = (i_z + 1, i_z + 1)$ for $\gamma = c$. Here the constant Π_γ is calculated to be 4.6×10^5 $\mu C/m^2$ for $\gamma = a$ and b, and 3.3×10^5 $\mu C/m^2$ for $\gamma = c$ from lattice parameters using the point-charge model.

In Fig. 3(a), we plot calculated P_S at $T \to 0$ as functions of J_b. Surprisingly we find a finite P_S in the ab spiral phase (e.g., $P_S \sim 500$ $\mu C/m^2$ for $J_b = 0.7$), while it is zero in the bc spiral phase. This can be understood as follows [see also Fig. 3(b)]. On the in-plane chains, the c-axis components of the DM vectors are arranged in the staggered way. As a result, the spin rotation angles in the ab spiral become subject to an alternate modulation [27]. Then the O ions between two spins with a smaller angle of $\phi - \Delta\phi$ (a larger angle of $\phi + \Delta\phi$) shift negatively (positively) to strengthen (weaken) the FM exchange through increasing (decreasing) the Mn-O-Mn bond angle. These shifts generate the ferroelectric polarization. In fact, the spin rotation angles in the bc spiral are also subject to the alternate modulation because of the staggered a-axis components of the DM vectors. However, the induced O shifts are opposite between neighboring ab planes, which results in their perfect cancellation.

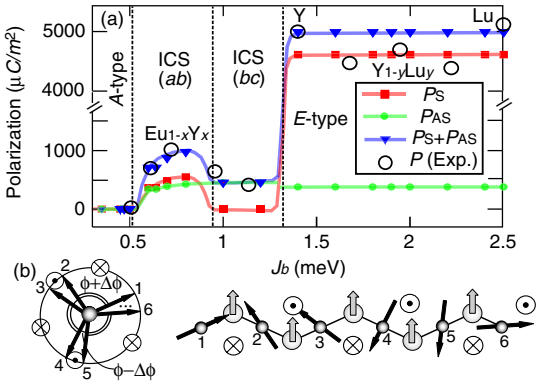

FIG. 3 (color online). (a) Polarizations vs J_b at $T \to 0$, i.e., $(\boldsymbol{S} \cdot \boldsymbol{S})$ contribution P_S, $(\boldsymbol{S} \times \boldsymbol{S})$ contribution P_{AS}, and experimentally measured P in $Eu_{1-x}Y_xMnO_3$ and $Y_{1-y}Lu_yMnO_3$ [9]. The summation $P_S + P_{AS}$ reproduces the experimental P well. (b) Alternation of the spin angles in the ab spiral state due to the staggered DM vectors is illustrated in an exaggerated manner where ⊙ (\otimes) denotes the positive (negative) c component of the vector. Shifts of the O ions due to the $(\boldsymbol{S} \cdot \boldsymbol{S})$-type magnetostriction are shown by gray arrows.

We also show J_b dependence of P_{AS} of $(\boldsymbol{S} \times \boldsymbol{S})$ origin at $T \to 0$ in Fig. 3(a). Since the P_{AS} consists of two contributions, i.e., the electronic and the lattice-mediated ones [26] and the former one is difficult to evaluate by the spin model, we calculate P_{AS} from the spin helicity $\boldsymbol{h}$. Note that P_{AS} is proportional to $|\boldsymbol{h}|$ and the observed P in the bc spiral phase is purely of $(\boldsymbol{S} \times \boldsymbol{S})$ origin. In addition, we plot the experimentally measured P of $Eu_{1-x}Y_xMnO_3$ and $Y_{1-y}Lu_yMnO_3$ for comparison [9], whose P originates purely from the Mn-spin order because of the absence of f moments [28]. Effective r_R and J_b of these solid solutions are evaluated by interpolations.

We find that the summation $P_S + P_{AS}$ reproduces well the experimental P. Here we emphasize that only the elastic constant K is an uncertain parameter in our model, and once we determine its value so as to reproduce the experimental P in the E phase, the behaviors of P in the spiral phases are reproduced almost perfectly. Moreover it turns out that the $(\boldsymbol{S} \cdot \boldsymbol{S})$ contribution P_S can be comparable to or even larger than the $(\boldsymbol{S} \times \boldsymbol{S})$ contribution P_{AS} in the ab spiral phase. This explains why P in the ab spiral phase is much larger than that in the bc spiral phase.

Next we discuss the E phase. Interestingly we find a finite c component of the spin-helicity vector $\boldsymbol{h}$ in this phase, indicating that its spin structure is not collinear in contrast to what we have believed so far, but its up-up-down-down structure is subject to a spiral modulation within the ab plane. The inset of Fig. 2 illustrates the real-space spin configuration of the E phase, which indeed shows the elliptically deformed ab-plane cycloid. Calculating the T dependence of the expectation value for each term in the Hamiltonian, we find that the single-ion anisotropy or alternation of the in-plane easy magnetization axes due to the $d_{3x^2-r^2}/d_{3y^2-r^2}$-type orbital ordering is an origin of the cycloidal deformation. This predicted deformation should be confirmed in a future polarized neutron-scattering experiment.

With dominant up-up-down-down spin b-axis components, the O ions between nearly (anti)parallel Mn-spin pairs shift negatively (positively) to modulate the FM exchanges, which results in the ferroelectric polarization (see inset of Fig. 2) [29,30]. In Fig. 3(a), we indeed see a very large P_S ($\sim$4600 $\mu C/m^2$) in the E phase. We also expect a small but finite $(\boldsymbol{S} \times \boldsymbol{S})$ contribution P_{AS} due to the cycloidal deformation. The calculated P_S, P_{AS} and their sum $P_S + P_{AS}$ in the E phase are invariant upon the J_b variation in agreement with the experiment [9].

Finally we discuss the coexistence of the E state and the IC-spiral (ICS) state. In the shaded area of Fig. 2, we obtain coexisting solutions when we perform the MC calculation starting from the ICS state as an initial configuration. The spin-phonon coupling or the $(\boldsymbol{S} \cdot \boldsymbol{S})$-type MS make the

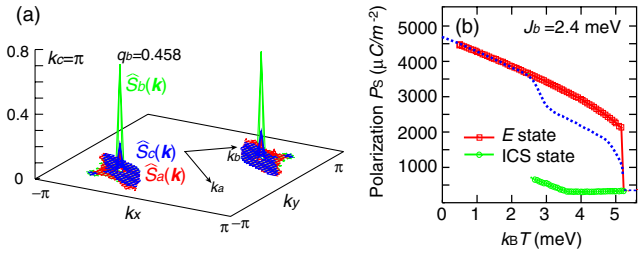

FIG. 4 (color online). (a) Calculated spin-correlation functions in the momentum space when the E and incommensurate spiral (ICS) states coexist. Here $\hat{S}_\gamma(\boldsymbol{k})$ denotes the correlation function for the spin γ-axis components. (b) Calculated T dependence of P_S in the pure E state and that in the ICS state for $2.6 < k_BT < 5.1$. Since the P_S in the coexisting regime necessarily becomes smaller than that for the pure E state, an anomaly can be observed in the T profile of P as indicated by the dashed line.

transition between ICS and E phases of strong first order. As a result, although the energy comparison gives the transition line between them as indicated by the solid line, the ICS state has a deep energy minimum even in the E phase. This can result in their coexistence. Such a coexistence easily occurs in reality since the system enters into the E phase necessarily via the IC sinusoidal collinear phase with lowering T.

To understand the contradicting neutron-scattering results [10–13], we calculate the spin-correlation functions in the momentum space for a coexisting solution obtained in the MC calculation. We find only the spin b-axis component has sharp peaks at $q_b = \pm 0.458$, while the other components have very small peaks as shown in Fig. 4(a). This seems as if the spin structure were IC *collinear*, which leads to the confusion. Observations of the IC $q_b \sim 0.43$ in $R\mathrm{MnO_3}$ with $R =$ Ho [11] and Er [13] as well as a report of the IC collinear state in $\mathrm{YMnO_3}$ [12] can be attributed to this coexisting state, while a report of the commensurate $q_b = 0.5$ in $\mathrm{HoMnO_3}$ [10] is to the pure E state.

When $1.8 < J_b < 2.5$, the energy minimum of the ICS state disappears as T decreases. In this case, an anomaly should appear in the T profile of P or dielectric constant [see Fig. 4(b)]. A recent experiment indeed observed such an anomaly in $\mathrm{YMnO_3}$ and $\mathrm{ErMnO_3}$ [9], which strongly evidences the coexistence. The coexistence together with the $(\boldsymbol{S}\cdot\boldsymbol{S})$ contribution in the E phase should be seriously considered also when we interpret the experimental results for $R\mathrm{MnO_3}$ with $R =$ Y, Ho, ..., Lu.

In summary, we have theoretically studied the magnetic structures and the ME coupling in $R\mathrm{MnO_3}$ by using a realistic spin model including the spin-phonon coupling. We have succeeded in reproducing the entire phase diagram of $R\mathrm{MnO_3}$ for the first time, and have revealed the cooperative contributions of symmetric $(\boldsymbol{S}\cdot\boldsymbol{S})$-type and antisymmetric $(\boldsymbol{S}\times\boldsymbol{S})$-type MSs to the ferroelectricity in the ab spiral phase. This mechanism is generic and is relevant to all the spin-spiral multiferroics. We have also found the cycloidal spin deformation in the E phase, and the coexistence of the E and ICS states. On these bases, the nontrivial behavior of $\boldsymbol{P}$ and several puzzles in the experiments have been explained. Our model gives a firm basis for studying and controlling the intriguing cross correlation phenomena in $R\mathrm{MnO_3}$.

The authors are grateful to Y. Tokura, S. Ishiwata, F. Kagawa, D. Okuyama, and T. Arima for discussions. This work was supported by Grant-in-Aids (22740214, 21244053, 17105002, 19048015, and 19048008), G-COE and NAREGI Project from MEXT Japan, and Funding Program for World-Leading Innovative R&D on Science and Technology (FIRST Program) from JSPS.

[1] M. Mochizuki and N. Furukawa, J. Phys. Soc. Jpn. **78**, 053704 (2009); Phys. Rev. B **80**, 134416 (2009).
[2] T. Kimura *et al.*, Nature (London) **426**, 55 (2003).
[3] For a recent review, Y. Tokura, J. Magn. Magn. Mater. **310**, 1145 (2007).
[4] T. Kimura *et al.*, Phys. Rev. B **71**, 224425 (2005).
[5] F. Kagawa *et al.*, Phys. Rev. Lett. **102**, 057604 (2009).
[6] F. Schrettle *et al.*, Phys. Rev. Lett. **102**, 207208 (2009).
[7] A. Pimenov *et al.*, Nature Phys. **2**, 97 (2006).
[8] N. Kida *et al.*, J. Opt. Soc. Am. B **26**, A35 (2009).
[9] S. Ishiwata *et al.*, Phys. Rev. B **81**, 100411(R) (2010).
[10] A. Munoz *et al.*, Inorg. Chem. **40**, 1020 (2001).
[11] H. W. Brinks *et al.*, Phys. Rev. B **63**, 094411 (2001).
[12] A. Munoz *et al.*, J. Phys. Condens. Matter **14**, 3285 (2002).
[13] F. Ye *et al.*, Phys. Rev. B **76**, 060402(R) (2007).
[14] M. Mochizuki, N. Furukawa, and N. Nagaosa, Phys. Rev. Lett. **104**, 177206 (2010).
[15] J. A. Alonso *et al.*, Inorg. Chem. **39**, 917 (2000).
[16] I. Solovyev, N. Hamada, and K. Terakura, Phys. Rev. Lett. **76**, 4825 (1996).
[17] The biquadratic term as an origin of the E phase is examined in T. A. Kaplan, Phys. Rev. B **80**, 012407 (2009).
[18] K. Hukushima and K. Nemoto, J. Phys. Soc. Jpn. **65**, 1604 (1996).
[19] To reproduce the observed V-shaped bicritical point for $\mathrm{Eu_{1-x}Y_xMnO_3}$ [9], we might have to consider the effect of randomness. Y. Tokura, Rep. Prog. Phys. **69**, 797 (2006).
[20] M. Kenzelmann *et al.*, Phys. Rev. Lett. **95**, 087206 (2005).
[21] Y. Yamasaki *et al.*, Phys. Rev. Lett. **101**, 097204 (2008).
[22] H. Katsura, N. Nagaosa, and A. V. Balatsky, Phys. Rev. Lett. **95**, 057205 (2005).
[23] I. A. Sergienko and E. Dagotto, Phys. Rev. B **73**, 094434 (2006).
[24] M. Mostovoy, Phys. Rev. Lett. **96**, 067601 (2006).
[25] Y. Yamasaki *et al.*, Phys. Rev. B **76**, 184418 (2007).
[26] A. Malashevich and D. Vanderbilt, Phys. Rev. Lett. **101**, 037210 (2008); Phys. Rev. B **80**, 224407 (2009).
[27] Note that the modulation is not caused by spin-spiral-induced small ferri-components of the DM vectors.
[28] The influence of rare-earth f moments is discussed in O. Prokhnenko *et al.*, Phys. Rev. Lett. **98**, 057206 (2007); **99**, 177206 (2007).
[29] I. A. Sergienko, C. Sen, and E. Dagotto, Phys. Rev. Lett. **97**, 227204 (2006).
[30] S. Picozzi *et al.*, Phys. Rev. Lett. **99**, 227201 (2007).